

# Undress to Redress: A Training-Free Framework for Virtual Try-On

Zhiying Li<sup>1</sup>, Junhao Wu<sup>3</sup>, Yeying Jin<sup>4</sup>, Daiheng Gao<sup>5</sup>, Yun Ji<sup>2</sup>, Kaichuan Kong<sup>1</sup>,  
Lei Yu<sup>6</sup>, Hao Xu<sup>7</sup>, Kai Chen<sup>7</sup>, Bruce Gu<sup>8</sup>, Nana Wang<sup>9</sup>, Zhaoxin Fan<sup>2</sup>

<sup>1</sup>Jinan University; <sup>2</sup>Beihang University; <sup>3</sup>Psyche AI Inc; <sup>4</sup>Tencent;

<sup>5</sup>University of Science and Technology of China; <sup>6</sup>Anhui University;

<sup>7</sup>Hong Kong University of Science and Technology; <sup>8</sup>Shandong Computer Science Center; <sup>9</sup>Eliza Lab

## Abstract

Virtual try-on (VTON) is a crucial task for enhancing user experience in online shopping by generating realistic garment previews on personal photos. Although existing methods have achieved impressive results, they struggle with long-sleeve-to-short-sleeve conversions—a common and practical scenario—often producing unrealistic outputs when exposed skin is underrepresented in the original image. We argue that this challenge arises from the “majority” completion rule in current VTON models, which leads to inaccurate skin restoration in such cases. To address this, we propose UR-VTON (Undress-Redress Virtual Try-ON), a novel, training-free framework that can be seamlessly integrated with any existing VTON method. UR-VTON introduces an “undress-to-redress” mechanism: it first reveals the user’s torso by virtually “undressing,” then applies the target short-sleeve garment, effectively decomposing the conversion into two more manageable steps. Additionally, we incorporate Dynamic Classifier-Free Guidance scheduling to balance diversity and image quality during DDPM sampling, and employ Structural Refiner to enhance detail fidelity using high-frequency cues. Finally, we present LS-TON, a new benchmark for long-sleeve-to-short-sleeve try-on. Extensive experiments demonstrate that UR-VTON outperforms state-of-the-art methods in both detail preservation and image quality. Code will be released upon acceptance.

## Introduction

Virtual try-on (VTON) realistically renders specified garments onto user-supplied images, significantly enhancing online shopping. However, existing methods focus on short-sleeve-to-short-sleeve or short-sleeve-to-long-sleeve transformations, common in summer and autumn, and perform poorly when users upload long-sleeve images yet seek to try on designated short sleeves during the spring–summer transition. These approaches often produce inaccurate garment replacements and introduce artifacts (see Fig. 1), severely limiting VTON’s practical utility and its ability to meet growing consumer demand for personalized, seamless shopping interactions. Thus, effective long-to-short sleeve conversion remains an urgent challenge.

Early VTON methods predominantly employed geometric deformation techniques, such as thin-plate splines (TPS)

Copyright © 2026, Association for the Advancement of Artificial Intelligence (www.aaai.org). All rights reserved.



Figure 1: Illustration of virtual try-on. Existing methods frequently fail to produce realistic results when transforming long-sleeve to short-sleeve. In contrast, our method achieves realistic virtual try-on with seamless transitions between long- and short- sleeve.

(Bookstein 2002; Ge et al. 2021a; Han et al. 2018) or optical-flow-based approaches (Bai et al. 2022; Ge et al. 2021b; He, Song, and Xiang 2022), but they often suffer from misalignment and fail to produce truly realistic garment swaps. Recently, inspired by the advances in conditional generative methods (Rombach et al. 2022; Li, Li, and Hoi 2023), a variety of new VTON approaches (Kim et al. 2024; Zhu et al. 2023; Yang et al. 2024) have emerged and achieved substantial improvements in visual quality. For instance, MGD (Baldtrati et al. 2023) introduce the first latent-space diffusion model for human fashion image editing, supporting multi-modal conditioning through text, pose, and sketch inputs; LaDI-VTON (Morelli et al. 2023) and StableVITON (Kim et al. 2024) adopt ControlNet (Zhang, Rao, and Agrawala 2023) architectures to encode supplementary information. DCI-VTON (Gou et al. 2023) casts virtual try-on as an image-inpainting task by incorporating the deformed garment as a local condition within the diffusion model. Sim-

ilarly, OOTDiffusion (Xu et al. 2025), IDM-VTON (Choi et al. 2024), and OutfitAnyone (Sun et al. 2024) utilize reference networks akin to denoising U-Nets (Ronneberger, Fischer, and Brox 2015) to generate new clothing appearances by processing garment regions. Despite these significant advances, existing methods still struggle with the common and practical challenge of converting long sleeves to short sleeves. We attribute this difficulty to the “majority” completion rule in current VTON models: if most pixels to be filled correspond to skin, the model correctly restores skin regions; but when the majority of the target region is clothing, it often erroneously completes skin areas with garment textures (as illustrated in Fig. 1). This limitation restricts VTON’s applicability to general scenarios and hinders accurate long-sleeve to short-sleeve try-on.

To address this challenge, we propose Undress-Redress Virtual Try-On (UR-VTON), a novel, training-free framework that can be seamlessly integrated with any existing VTON model. At the core of our approach is an “undress-to-redress” mechanism: we first undress the long-sleeved garment to reveal the torso, and then redress it with the target short-sleeved garment. By decomposing the challenging one-step transformation from long sleeves to short sleeves into two manageable stages, our method substantially improves both accuracy and consistency. To further enhance performance, we introduce a dynamic classifier-free guidance scheduler, which addresses the limitations of using a fixed guidance scale in DDPM sampling (Ho, Jain, and Abbeel 2020)—a common issue that often struggles to balance diversity and image quality (Malarz et al. 2025). Complementing this, we present a structural refiner strategy that leverages high-frequency structural cues from the input image at the final output stage, further enhancing visual fidelity. To facilitate comprehensive evaluation, we also introduce LS-TON, a novel benchmark specifically designed for long-sleeve-to-short-sleeve try-on scenarios. Extensive experiments demonstrate that UR-VTON achieves state-of-the-art results, yielding significant gains in detail preservation and overall image quality. In summary, our contribution can be summarized as:

- We propose UR-VTON, a novel, training-free framework that can be seamlessly integrated with any existing VTON model. By employing an undress-to-redress mechanism, it decomposes the complex, one-step task of converting long sleeves to short sleeves into simpler, controllable steps.
- We employ a dynamic classifier-free guidance schedule to balance diversity and image quality during DDPM sampling, and utilize structural refiner to enhance detail fidelity by leveraging high-frequency structural cues.
- We present LS-TON, a novel benchmark comprising 770 image triplets, each consisting of a model with long-sleeve, the corresponding short-sleeved garment, and the model with short-sleeve, for evaluating long-sleeve-to-short-sleeve try-on performance.
- Extensive experiments demonstrate that UR-VTON attains state-of-the-art performance, yielding substantial improvements in detail preservation and overall image

quality, and validating its practical applicability.

## Related Work

### Image-based Virtual Try-On

Image-based virtual try-on aims to generate images of a person wearing a target garment while retaining texture details and identity. Typically, methods consist of two stages: garment warping and fusion. Early methods used Thin-Plate Spline (TPS) (Bookstein 2002) for geometric deformation (Ge et al. 2021a; Yang et al. 2020; Han et al. 2018), whereas recent optical flow approaches (Bai et al. 2022; Ge et al. 2021b; He, Song, and Xiang 2022) improve non-rigid alignment but remain prone to estimation errors. Fusion techniques can be divided into GAN- and diffusion-based approaches. GAN-based methods (Lee et al. 2022; Lewis, Varadharajan, and Kemelmacher-Shlizerman 2021; Morelli et al. 2022) demonstrate strong potential but suffer from unstable training (Gulrajani et al. 2017) and mode collapse (Miyato et al. 2018), harming image quality. Diffusion-based methods (Kim et al. 2024; Zhu et al. 2023; Yang et al. 2024) provide more stable training and superior quality with enhanced coverage and flexibility. TryOnDiffusion (Zhu et al. 2023) uses dual UNets (Ronneberger, Fischer, and Brox 2015) to integrate clothing, body, and pose. LaDI-VTON (Morelli et al. 2023) aligns garment features with CLIP (Radford et al. 2021) embeddings and refines diffusion via warped inputs. GP-VTON (Xie et al. 2023) applies part-wise warping to maintain semantic consistency and texture fidelity. OOTDiffusion (Xu et al. 2025) fine-tunes a pre-trained garment UNet within the denoising UNet for detailed learning. IDM-VTON (Choi et al. 2024) merges IP-Adapter (Ye et al. 2023) semantics through cross-attention and employs parallel UNets for refinement. CatVTON (Chong et al. 2025) simplifies UNet via spatial concatenation, achieving high quality with 899.06 M parameters (49.57 M trainable). Leffa (Zhou et al. 2025) embeds flow-field learning regularization into the diffusion model’s attention layers to align target queries with reference-image regions. This reduces fine-grained distortions and preserves high-quality results in virtual try-on.

Despite these advances, existing methods struggle with long-sleeve to short-sleeve transformations. We propose a simple, effective, training-free universal framework to address this challenge via task decomposition.

### Classifier-Free Guidance and Structural Refiner

Classifier-Free Guidance (CFG) (Ho and Salimans 2022) enhances sample quality and controllability in diffusion models and underpins systems like Stable Diffusion (Rombach et al. 2022), DALL·E 2 (Ramesh et al. 2022), and Imagen (Saharia et al. 2022). CFG is trained by randomly omitting conditioning signals, enabling the model to predict both conditional and unconditional noise. At inference, these predictions are combined as:

$$\varepsilon_{\text{uncond}} = \varepsilon_{\theta}(z_t), \quad \varepsilon_{\text{cond}} = \varepsilon_{\theta}(z_t|y), \quad (1)$$

$$\varepsilon_{\text{cfg}} = \varepsilon_{\text{uncond}} + \omega(\varepsilon_{\text{cond}} - \varepsilon_{\text{uncond}}), \quad (2)$$

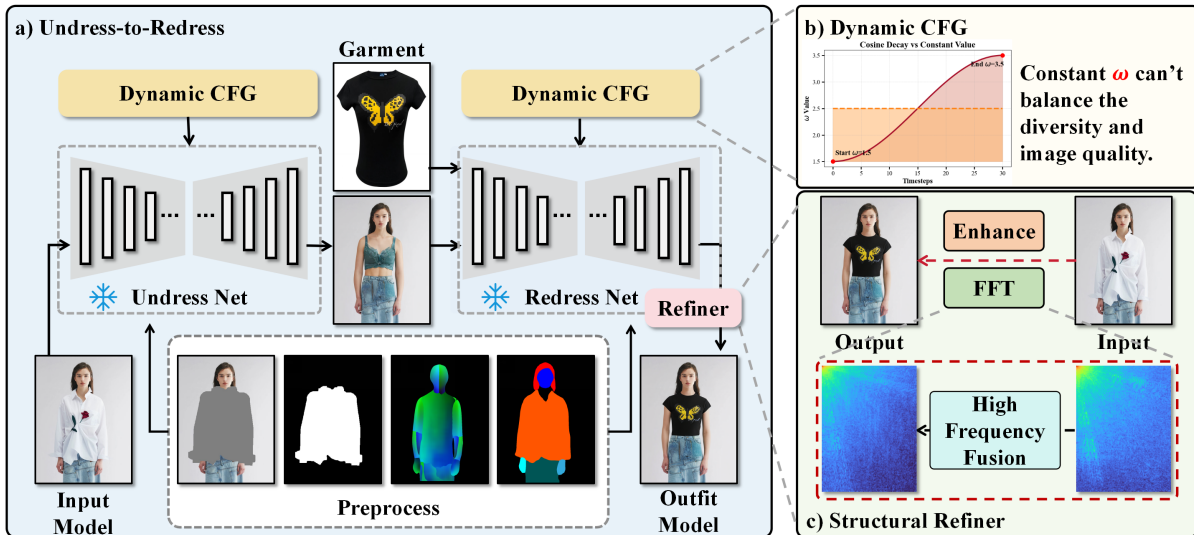


Figure 2: Overview of the proposed UR-VTON framework. **a)** UR-VTON employs an “Undress-to-Redress” mechanism: it first undresses the long-sleeved garment to expose the torso and then redresses the target short-sleeved garment. **b)** Dynamic CFG scheduler is incorporated into the diffusion process to balance diversity and image quality. **c)** Structural Refiner leverages high-frequency structural cues from the input image at the final output stage to further enhance visual fidelity.

where  $\omega$  denotes the guidance scale,  $z_t$  represents the latent vector at time step  $t$ .  $\varepsilon_{\text{uncond}}$  and  $\varepsilon_{\text{cond}}$  respectively refer to the noise predicted by the model’s forward diffusion process under an empty prompt and under the conditioning prompt  $y$ . This mechanism balances fidelity and diversity without an external classifier. Virtual try-on methods (Choi et al. 2024; Chong et al. 2025; Zhou et al. 2025) typically use CFG with  $\omega = 2.5$  to maintain texture fidelity and realism, but a fixed scale may not suit specialized tasks (Shen et al. 2024; Li et al. 2025). We thus propose Dynamic CFG to adaptively adjust  $\omega$  during sampling.

Recent studies integrate frequency-domain knowledge into image enhancement to better restore details and structure (Chen, Duanmu, and Long 2024; Ma et al. 2024). For example, Fuoli et al. (Fuoli, Van Gool, and Timofte 2021) introduce a Fourier-domain perceptual loss to maintain high-frequency consistency and sharpen edges and textures in super-resolved images. Zhou et al. (Zhou et al. 2022) propose a spatial–frequency fusion network that jointly extracts and fuses spatial and frequency features to enhance global and local representations, significantly improving pan-sharpening performance. Building on these works, we leverage structural cues from the input image’s frequency domain to further improve output quality.

### LS-TON Benchmark

The widely used public virtual try-on datasets, such as VITON-HD (Choi et al. 2021) and DressCode (Morelli et al. 2022), lack data specifically designed for the long-sleeve to short-sleeve garment transfer task, most instances involve short-sleeve to short-sleeve transformations, as depicted in Fig. 3(a). Consequently, these datasets are insufficient for effectively evaluating the performance of VTON models

on the more challenging long-sleeve to short-sleeve scenario. To bridge this gap, we introduce a novel benchmark, LS-TON, tailored for long-sleeve to short-sleeve transfer. We curated image pairs from social platforms, consisting of models dressed in long-sleeved garments (e.g., heavy coats, padded jackets, and long-sleeved shirts) and corresponding short-sleeved clothing. Using a variety of image editing tools, we manually replace the long sleeves on the models with short sleeves, resulting in image triplets: the source image (the model in long sleeves), the reference image (the short-sleeved garment), and the ground-truth image (the model in short sleeves), as shown in Fig. 3(b). LS-TON comprises 770 such triplets.

## Method

We aim to achieve seamless and realistic virtual try-on of short-sleeved garments for models originally dressed in long-sleeved clothing. To this end, we introduce UR-VTON, a training-free framework capable of integrating any VTON model. As illustrated in Fig. 2, UR-VTON comprises three key components: an “Undress-to-Redress” module, Dynamic Classifier-Free Guidance (DCFG) for diffusion process, and Structural Refiner to enhance output quality. Next, we present the detailed description.

### Undress-to-Redress

Existing VTON models face a practical challenge in transforming long sleeves to short sleeves, owing to the “majority” rule: when most pixels in the target region correspond to skin, the model accurately reconstructs skin; however, when clothing pixels predominate, it often misrepresents skin areas as clothing textures (see Fig. 1). This issue



Figure 3: The overview of virtual try-on datasets. (a) Existing datasets such as VITON-HD and DressCode lack data for long-sleeve to short-sleeve transformations. (b) LS-TON is a dataset specifically constructed for long-sleeve to short-sleeve garment virtual try-on.

limits VTON’s applicability in general scenarios and undermines the precision of long-to-short sleeve conversions.

To address this, we propose an “Undress-to-Redress” mechanism, which decomposes the long-sleeve to short-sleeve transformation into two sequential stages (see Fig. 2 (a)): “intermediate body exposure” and “final garment overlay”. In the first stage, an intermediate result is generated with greater torso visibility. Formulation is as follows:

$$\varepsilon_{\theta}^1 = \text{UNet}([z_t^1, G^1, M, D], t), \quad (3)$$

$$\varepsilon_{\text{cond}}^1, \varepsilon_{\text{uncond}}^1 = \text{Chunk}(\varepsilon_{\theta}^1), \quad (4)$$

$$\varepsilon_{\text{cfg}}^1 = \varepsilon_{\text{uncond}}^1 + \omega(\varepsilon_{\text{cond}}^1 - \varepsilon_{\text{uncond}}^1), \quad (5)$$

$$z_{t-1}^1 = \frac{1}{\sqrt{\alpha_t}}(z_t^1 - \frac{1 - \alpha_t}{\sqrt{1 - \bar{\alpha}_t}}\varepsilon_{\text{cfg}}^1) + \sigma_t\varepsilon', \quad (6)$$

where  $z_t^1$  is the latent representation from forward diffusion.  $G^1$  is the reference image for replacement (we choose the bra).  $M$  and  $D$  denote the binary mask of source image and DensePose, respectively.  $t$  is the time step.  $\alpha_t$  and  $\bar{\alpha}_t$  are forward diffusion retention coefficients.  $\sigma_t$  is the noise standard deviation from the scheduler.  $\varepsilon' \sim \mathcal{N}(0, I)$ . Chunk represents the average operation on the batch dimension. The guidance scale  $\omega$  is often empirically set to 2.5.

Similarly, in the next stage, the user-provided reference image of the short-sleeved garment  $G^2$  is virtually applied

to the intermediate image. The formulation is as follows:

$$\varepsilon_{\theta}^2 = \text{UNet}([z_t^2, G^2, M, D], t), \quad (7)$$

$$\varepsilon_{\text{cond}}^2, \varepsilon_{\text{uncond}}^2 = \text{Chunk}(\varepsilon_{\theta}^2), \quad (8)$$

$$\varepsilon_{\text{cfg}}^2 = \varepsilon_{\text{uncond}}^2 + \omega(\varepsilon_{\text{cond}}^2 - \varepsilon_{\text{uncond}}^2), \quad (9)$$

$$z_{t-1}^2 = \frac{1}{\sqrt{\alpha_t}}(z_t^2 - \frac{1 - \alpha_t}{\sqrt{1 - \bar{\alpha}_t}}\varepsilon_{\text{cfg}}^2) + \sigma_t\varepsilon', \quad (10)$$

where  $z_t^2$  is the latent representation from forward diffusion on the intermediate image.

The rationale for this two-stage approach is that direct transformation from long sleeves to short sleeves is often intractable. By first generating an image with the model dressed only in undergarments, the arms and shoulders become clearly visible, thus alleviating the need for the model to simultaneously render both the torso and garment regions.

### Dynamic Classifier-Free Guidance

Classifier-Free Guidance (CFG) (Ho and Salimans 2022) is a technique for adjusting the intensity of conditional signals in diffusion models without requiring an additional classifier. At each denoising step, CFG linearly combines noise predictions from conditional and unconditional models, enabling a controllable trade-off between sample fidelity and diversity. However, existing VTON models typically use a fixed weighting coefficient throughout all denoising steps. Although this ensures stable guidance, it frequently results in excessive guidance at early stages and insufficient guidance at later stages, introducing unwanted artifacts (Kynkäänniemi et al. 2024). To address this issue, we propose Dynamic CFG, in Fig. 2 (b), inspired by (Malarz et al. 2025), which employs dynamic weighting coefficients to adaptively control the conditional signal strength. This approach preserves diversity during the initial stages and enhances output quality at later stages. Taking the first stage as an example, the formulation is presented as follows:

$$\omega_{\text{dfg}} = \omega - \cos(\pi \times \frac{t}{T-1}), \quad (11)$$

$$\varepsilon_{\text{cfg}}^1 = \varepsilon_{\text{uncond}}^1 + \omega_{\text{dfg}}(\varepsilon_{\text{cond}}^1 - \varepsilon_{\text{uncond}}^1), \quad (12)$$

where  $t$  represents the current timestep, and  $T$  indicates the total number of timesteps.

### Structural Refiner

To further enhance the edge structures in the virtual try-on results, in Fig. 2 (c), we incorporate the structural information of the input image  $P(x, y)$  into the generated output  $R(x, y)$ , thus improving the quality of the synthesis. Specifically, we first apply the Fourier transform to convert both  $P(x, y)$  and  $R(x, y)$  into the frequency domain:

$$\mathcal{K}_P(u, v) = \mathcal{F}\{P(x, y)\}(u, v), \quad (13)$$

$$\mathcal{K}_R(u, v) = \mathcal{F}\{R(x, y)\}(u, v), \quad (14)$$

where  $(x, y)$  denotes the spatial coordinates of image pixels, while  $(u, v)$  represents the corresponding frequency components.  $\mathcal{F}$  refers to the two-dimensional discrete Fourier transform.

Subsequently, the magnitude and phase components are separated:

$$\mathcal{A}_P(u, v) = |\mathcal{K}_P(u, v)|, \quad (15)$$

$$\mathcal{A}_R(u, v) = |\mathcal{K}_R(u, v)|, \quad \Phi_R(u, v) = \angle \mathcal{K}_R(u, v). \quad (16)$$

We apply a high-frequency mask  $\mathcal{B}(u, v)$  to fuse the amplitude  $\mathcal{A}_P(u, v)$  into  $\mathcal{A}_R(u, v)$  in the high-frequency regions. The resulting amplitude is then combined with the phase spectrum  $\Phi_R(u, v)$  to form a complex frequency-domain representation, as formulated below:

$$\mathcal{A}_{\hat{R}}(u, v) = [1 - \mathcal{B}(u, v)]\mathcal{A}_R(u, v) + \frac{\mathcal{B}(u, v) [\mathcal{A}_P(u, v) + \mathcal{A}_R(u, v)]}{2}, \quad (17)$$

$$\mathcal{K}_{\hat{R}}(u, v) = \mathcal{A}_{\hat{R}}(u, v) \exp(j\Phi_R(u, v)), \quad (18)$$

where  $j$  denotes the imaginary unit.

This composite frequency representation is transformed back into the spatial domain using the inverse Fourier transform, producing an image with enhanced edges  $\hat{R}(x, y) = \mathcal{F}^{-1} \{ \mathcal{K}_{\hat{R}}(u, v) \} (x, y)$ .

## Experiments

### Experimental Settings

**Datasets.** We conduct experiments on two public fashion datasets, VITON-HD (Choi et al. 2021) and DressCode (Morelli et al. 2022), and a custom benchmark (LS-TON) for long-sleeve to short-sleeve try-on evaluation. VITON-HD contains 13,679 image pairs (11,647 training; 2,032 testing), each comprising a front-view upper-body photograph and its corresponding in-shop top at  $1024 \times 768$  resolution. DressCode contains 48,392 training and 5,400 testing pairs of full-body, front-view images paired with in-shop garments (tops, bottoms, and dresses), also at  $1024 \times 768$  resolution. LS-TON includes 770 triplets: a person wearing a long-sleeved garment, the matching in-shop short-sleeved garment, and the person wearing the short-sleeved version. The long-sleeved garments span thick coats, hoodies, and padded jackets. All LS-TON data follow the VITON-HD preprocessing protocol.

**Baselines.** We benchmark our proposed UR-VTON against several state-of-the-art diffusion-based virtual try-on models, including: GP-VTON (Xie et al. 2023) (part-wise garment warping for semantic and texture fidelity), LaDI-VTON (Morelli et al. 2023) (CLIP-based feature alignment and diffusion refinement), IDM-VTON (Choi et al. 2024) (cross-attention and parallel UNets for detail), OOTDiffusion (Xu et al. 2025) (fine-tuned garment UNet for denoising), CatVTON (Chong et al. 2025) (UNet simplification via spatial concatenation), and Leffa (Zhou et al. 2025) (attention flow regularization for artifact reduction and efficient portrait generation).

**Evaluation Metrics.** To ensure fair evaluation of our model, we follow the established VTON evaluation protocol. In the paired try-on setting with ground truth from the test dataset, we employ four widely used metrics to assess the similarity between synthesized and real images: Structural Similarity

Methods	LS-TON						
	Backbone	Paired				Unpaired	
		SSIM $\uparrow$	FID $\downarrow$	KID $\downarrow$	LPIPS $\downarrow$	FID $\downarrow$	KID $\downarrow$
LaDI-VTON [2023 ACM MM]	-	0.768	47.848	23.863	0.206	50.593	26.120
IDM-VTON [2024 ECCV]	-	0.750	43.311	14.752	0.247	46.601	19.923
OOTDiffusion [2025 AAAI]	-	0.775	50.615	24.762	0.199	50.775	23.460
CatVTON [2025 ICLR]	-	0.760	40.702	11.736	0.227	41.401	11.866
Leffa [2025 CVPR]	-	0.755	41.398	13.405	0.234	45.557	14.001
<b>UR-VTON</b>	CatVTON	<u>0.804</u>	<u>31.315</u>	<u>8.038</u>	<u>0.154</u>	<u>33.094</u>	<u>9.090</u>
<b>UR-VTON</b>	Leffa	<b>0.811</b>	<b>31.074</b>	<b>7.723</b>	<b>0.169</b>	<b>32.866</b>	<b>8.322</b>

Table 1: Quantitative comparison on LS-TON. The best and the second best-results are **highlighted** and underlined.

Index (SSIM) (Wang et al. 2004), Learned Perceptual Image Patch Similarity (LPIPS) (Zhang et al. 2018), Fréchet Inception Distance (FID) (Seitzer 2020), and Kernel Inception Distance (KID) (Bińkowski et al. 2018). In the unpaired setting, we use FID and KID to evaluate the distributional similarity between generated and real samples.

**Implementation Details.** The experiments are conducted on an Ubuntu 20.04.6 LTS system with the PyTorch framework, a single NVIDIA L20 GPU, and 45 GB of RAM. Unless otherwise specified, Leffa is used as the backbone for UR-VTON in all subsequent experimental settings. The total number of timesteps  $T = 30$ , and guidance scale  $\omega = 2.5$ .

### Quantitative Comparison

To comprehensively evaluate the performance of UR-VTON, we conduct quantitative comparisons with state-of-the-art models on the VITON-HD, DressCode, and our proprietary LS-TON datasets. Experiments are performed under both paired and unpaired settings to assess not only the similarity between synthesized images and ground truth, but also the models’ generalization capabilities. Notably, as UR-VTON can integrate arbitrary VTON backbones, we implemented both CatVTON and Leffa as its backbone in this experiment settings. Table 1 shows that UR-VTON significantly outperforms all baseline methods across every metric on LS-TON, demonstrating the effectiveness of the UR-VTON model architecture and the “undress-to-redress” strategy in long-sleeve to short-sleeve conversions. Additionally, we evaluate UR-VTON on VITON-HD and DressCode to observe its ability in general scenarios. As reported in Table 2, UR-VTON still achieves the best or second-best results on most metrics, further confirming its superiority. Notably, Leffa achieves competitive results on VITON-HD, especially in terms of the KID metric. We attribute this to the nature of the KID score, which predominantly measures distributional differences between generated outputs and ground truth. Since UR-VTON requires additional torso reconstruction during synthesis, the distribution calculations over the generated torso area may lead to higher KID values. In contrast, Leffa focuses solely on the garment region and does not involve torso reconstruction.

### Qualitative Comparison

To further demonstrate the effectiveness of UR-VTON, we conduct a qualitative evaluation of its virtual try-on results via visual analysis in long-sleeve to short-sleeve garment conversion tasks. As illustrated in Fig. 4, we showcase chal-

Methods		VITON-HD						DressCode					
		Paired				Unpaired		Paired				Unpaired	
Models	Backbone	SSIM $\uparrow$	FID $\downarrow$	KID $\downarrow$	LPIPS $\downarrow$	FID $\downarrow$	KID $\downarrow$	SSIM $\uparrow$	FID $\downarrow$	KID $\downarrow$	LPIPS $\downarrow$	FID $\downarrow$	KID $\downarrow$
GP-VTON [2023 CVPR]	-	<u>0.891</u>	6.539	1.097	0.069	9.628	1.298	<b>0.922</b>	7.466	5.738	0.070	10.064	8.035
LaDI-VTON [2023 ACM MM]	-	0.864	11.211	7.006	0.073	14.418	8.422	0.895	7.280	4.479	0.057	9.402	5.421
IDM-VTON [2024 ECCV]	-	<b>0.899</b>	5.762	0.732	0.079	9.842	2.134	<u>0.904</u>	5.165	2.553	0.072	6.941	2.979
OOTDiffusion [2025 AAAI]	-	0.842	6.236	0.770	0.086	9.341	1.018	0.886	5.341	2.372	0.090	8.929	4.399
CatVTON [2025 ICLR]	-	0.835	6.389	0.894	0.070	9.050	1.181	0.877	4.049	<u>0.981</u>	<u>0.053</u>	6.137	1.403
Leffa [2025 CVPR]	-	0.8566	<b>5.261</b>	<b>0.154</b>	<u>0.063</u>	<b>8.357</b>	<b>0.227</b>	0.893	5.130	1.941	0.107	6.370	2.309
<b>UR-VTON</b>	CatVTON	0.869	5.676	0.547	<b>0.060</b>	9.275	1.496	0.902	<b>3.214</b>	<b>0.644</b>	<b>0.042</b>	<b>5.207</b>	<b>1.300</b>
<b>UR-VTON</b>	Leffa	0.844	6.218	<u>0.531</u>	0.077	<u>9.028</u>	<u>0.689</u>	0.883	5.334	2.188	0.119	7.001	2.593

Table 2: Quantitative comparison on VITON-HD and DressCode. The best and the second-best results are **highlighted** and underlined.

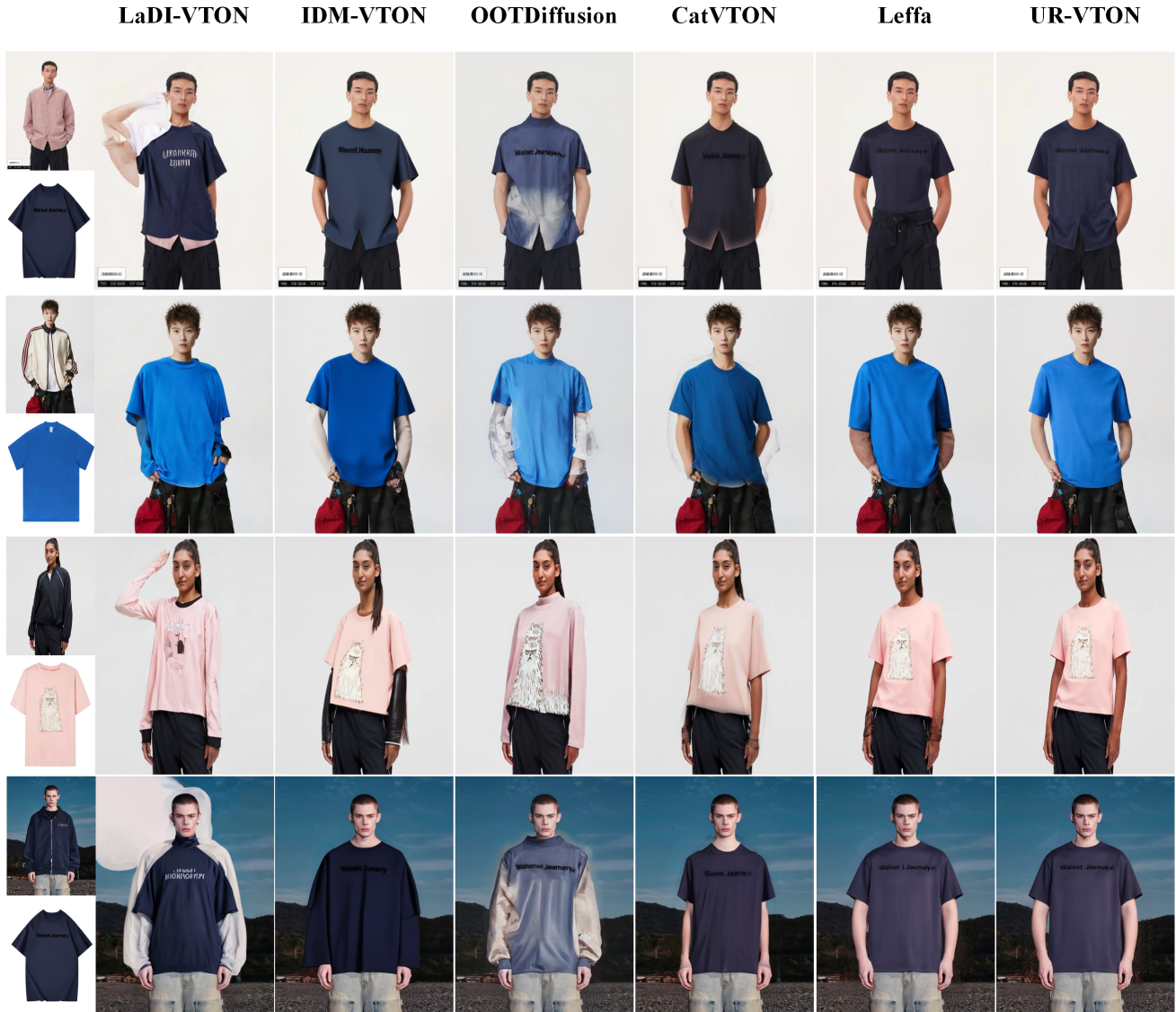


Figure 4: **Qualitative comparison on the LS-TON dataset.** UR-VTON demonstrates significant advantages when handling the challenging task of converting long-sleeve to short-sleeve garment transition scenarios. Please zoom in to view more details.



Figure 5: **Qualitative comparison of UR-VTON in real-world long-sleeve-to-short-sleeve garment transitions.** Please zoom in to view more details. “GT” denotes the ground-truth.

Methods	Paired				Unpaired	
	SSIM $\uparrow$	FID $\downarrow$	KID $\downarrow$	LPIPS $\downarrow$	FID $\downarrow$	KID $\downarrow$
Original	0.755	41.398	13.405	0.234	45.557	14.001
+ UR	0.795	33.538	8.796	0.186	34.487	9.896
+ DCFG	0.762	41.195	11.885	0.229	44.741	12.946
+ SR	0.759	41.288	12.694	0.230	45.018	13.529
<b>UR-VTON</b>	<b>0.811</b>	<b>31.074</b>	<b>7.723</b>	<b>0.169</b>	<b>32.866</b>	<b>8.322</b>

Table 3: Ablation study on LS-TON. The best results are **highlighted**. “UR” represents the Undress-to-Redress mechanism. “DCFG” represents the dynamic classifier-free guidance. “SR” represents the structural refiner.

lenging sleeve transformation results on the LS-TON dataset and compare multiple state-of-the-arts methods to highlight differences in fine-grained consistency. Notably, alternative approaches often exhibit incorrect garment transfer, visual artifacts, chaotic outputs, and detail loss, which substantially limit their real-world applicability. In contrast, UR-VTON consistently produces accurate and natural garment transfers, further highlighting its superior generalization capability and practical utility.

### Ablation Study

We conduct ablation studies on the LS-TON dataset to assess the contribution of each module to UR-VTON’s performance in long-sleeve-to-short-sleeve garment conversion. As shown in Table 3, the model employing only the “Undress-to-Redress” (UR) mechanism exhibits a substantial improvement over the original model. In contrast, using dynamic classifier-free guidance (DCFG) or structural refiner (SR) alone results in only modest gains. Ultimately, the UR-VTON model, which integrates UR, DCFG, and SR, achieves the highest performance. This outcome is antic-

ipated, as the UR mechanism offers an intermediate representation with increased torso exposure, significantly reducing task complexity and enabling marked performance enhancements. DCFG and SR primarily serve to refine the fine-grained details of the try-on outputs. The integration of these three modules provides comprehensive and stable global information, thereby offering strong support for virtual try-on systems.

### Application

To assess the practical effectiveness of UR-VTON, we recruited several participants as models and photographed them in both long-sleeved and short-sleeved garments using a mobile device, with an emphasis on maintaining consistent poses. The collected images are subsequently processed by the VTON models. As illustrated in Fig. 5, UR-VTON demonstrated superior virtual try-on performance, producing highly accurate results. By contrast, alternative methods failed to achieve precise garment transfer, further substantiating the practical advantages of UR-VTON.

### Conclusion

This paper introduces a novel training-free virtual try-on (VTON) framework, UR-VTON, which utilizes an “Undress-to-Redress” mechanism alongside two detail refinement strategies to address the challenge of transferring from long-sleeved to short-sleeved garments. By decomposing the process into sequential steps, the proposed method effectively prevents unrealistic image generation resulting from insufficient torso exposure in direct synthesis. Moreover, the integration of fine-grained information mitigates artifacts that may emerge during multiple inference stages. To effectively assess the performance of VTON models for this specific task, we construct a novel benchmark dataset,

LS-TON, dedicated to the long-sleeve-to-short-sleeve garment transition. Experimental results demonstrate that UR-VTON consistently outperforms existing methods across diverse datasets and tasks. Additionally, application confirms that UR-VTON is highly practical and exhibits strong applicability in real-world scenarios.

## References

- Bai, S.; Zhou, H.; Li, Z.; Zhou, C.; and Yang, H. 2022. Single stage virtual try-on via deformable attention flows. In *European Conference on Computer Vision*, 409–425.
- Baldrati, A.; Morelli, D.; Cartella, G.; Cornia, M.; Bertini, M.; and Cucchiara, R. 2023. Multimodal garment designer: Human-centric latent diffusion models for fashion image editing. In *International Conference on Computer Vision*, 23393–23402.
- Bińkowski, M.; Sutherland, D. J.; Arbel, M.; and Gretton, A. 2018. Demystifying mmd gans. *arXiv preprint arXiv:1801.01401*.
- Bookstein, F. L. 2002. Principal warps: Thin-plate splines and the decomposition of deformations. *IEEE Transactions on Pattern Analysis and Machine Intelligence*, 11(6): 567–585.
- Chen, J.; Duanmu, C.; and Long, H. 2024. Large kernel frequency-enhanced network for efficient single image super-resolution. In *Computer Vision and Pattern Recognition*, 6317–6326.
- Choi, S.; Park, S.; Lee, M.; and Choo, J. 2021. Viton-hd: High-resolution virtual try-on via misalignment-aware normalization. In *Computer Vision and Pattern Recognition*, 14131–14140.
- Choi, Y.; Kwak, S.; Lee, K.; Choi, H.; and Shin, J. 2024. Improving diffusion models for authentic virtual try-on in the wild. In *European Conference on Computer Vision*, 206–235.
- Chong, Z.; Dong, X.; Li, H.; Zhang, S.; Zhang, W.; Zhang, X.; Zhao, H.; Jiang, D.; and Liang, X. 2025. Catvton: Concatenation is all you need for virtual try-on with diffusion models. In *International Conference on Learning Representations*.
- Clancey, W. J. 1979. *Transfer of Rule-Based Expertise through a Tutorial Dialogue*. Ph.D. diss., Dept. of Computer Science, Stanford Univ., Stanford, Calif.
- Clancey, W. J. 1983. Communication, Simulation, and Intelligent Agents: Implications of Personal Intelligent Machines for Medical Education. In *Proceedings of the Eighth International Joint Conference on Artificial Intelligence (IJCAI-83)*, 556–560. Menlo Park, Calif: IJCAI Organization.
- Clancey, W. J. 1984. Classification Problem Solving. In *Proceedings of the Fourth National Conference on Artificial Intelligence*, 45–54. Menlo Park, Calif.: AAAI Press.
- Clancey, W. J. 2021. The Engineering of Qualitative Models. Forthcoming.
- Engelmore, R.; and Morgan, A., eds. 1986. *Blackboard Systems*. Reading, Mass.: Addison-Wesley.
- Fuoli, D.; Van Gool, L.; and Timofte, R. 2021. Fourier space losses for efficient perceptual image super-resolution. In *International Conference on Computer Vision*, 2360–2369.
- Ge, C.; Song, Y.; Ge, Y.; Yang, H.; Liu, W.; and Luo, P. 2021a. Disentangled cycle consistency for highly-realistic virtual try-on. In *Computer Vision and Pattern Recognition*, 16928–16937.
- Ge, Y.; Song, Y.; Zhang, R.; Ge, C.; Liu, W.; and Luo, P. 2021b. Parser-free virtual try-on via distilling appearance flows. In *Computer Vision and Pattern Recognition*, 8485–8493.
- Gou, J.; Sun, S.; Zhang, J.; Si, J.; Qian, C.; and Zhang, L. 2023. Taming the power of diffusion models for high-quality virtual try-on with appearance flow. In *ACM International Conference on Multimedia*, 7599–7607.
- Gulrajani, I.; Ahmed, F.; Arjovsky, M.; Dumoulin, V.; and Courville, A. C. 2017. Improved training of wasserstein gans. *Advances in Neural Information Processing Systems*, 30.
- Han, X.; Wu, Z.; Wu, Z.; Yu, R.; and Davis, L. S. 2018. Viton: An image-based virtual try-on network. In *Computer Vision and Pattern Recognition*, 7543–7552.
- Hasling, D. W.; Clancey, W. J.; and Rennels, G. 1984. Strategic explanations for a diagnostic consultation system. *International Journal of Man-Machine Studies*, 20(1): 3–19.
- Hasling, D. W.; Clancey, W. J.; Rennels, G. R.; and Test, T. 1983. Strategic Explanations in Consultation—Duplicate. *The International Journal of Man-Machine Studies*, 20(1): 3–19.
- Hassibi, B.; Stork, D. G.; and Wolff, G. J. 1993. Optimal brain surgeon and general network pruning. In *IEEE International Conference on Neural Networks*, 293–299.
- He, S.; Song, Y.-Z.; and Xiang, T. 2022. Style-based global appearance flow for virtual try-on. In *Computer Vision and Pattern Recognition*, 3470–3479.
- Ho, J.; Jain, A.; and Abbeel, P. 2020. Denoising diffusion probabilistic models. *Advances in Neural Information Processing Systems*, 33: 6840–6851.
- Ho, J.; and Salimans, T. 2022. Classifier-free diffusion guidance. *arXiv*.
- Kim, J.; Gu, G.; Park, M.; Park, S.; and Choo, J. 2024. Stableviton: Learning semantic correspondence with latent diffusion model for virtual try-on. In *Computer Vision and Pattern Recognition*, 8176–8185.
- Kynkäänniemi, T.; Aittala, M.; Karras, T.; Laine, S.; Aila, T.; and Lehtinen, J. 2024. Applying guidance in a limited interval improves sample and distribution quality in diffusion models. *Advances in Neural Information Processing Systems*, 37: 122458–122483.
- Lee, S.; Gu, G.; Park, S.; Choi, S.; and Choo, J. 2022. High-resolution virtual try-on with misalignment and occlusion-handled conditions. In *European Conference on Computer Vision*, 204–219.
- Lewis, K. M.; Varadharajan, S.; and Kemelmacher-Shlizerman, I. 2021. Tryongan: Body-aware try-on via layered interpolation. *ACM Transactions on Graphics*, 40(4): 1–10.

- Li, D.; Li, J.; and Hoi, S. 2023. Blip-diffusion: Pre-trained subject representation for controllable text-to-image generation and editing. *Advances in Neural Information Processing Systems*, 36: 30146–30166.
- Li, P.; Yan, S.; Tsai, J.; Zhang, R.; An, R.; Guo, Z.; and Gao, X. 2025. Adaptive Classifier-Free Guidance via Dynamic Low-Confidence Masking. *arXiv preprint arXiv:2505.20199*.
- Ma, R.; Zhang, Y.; Zhang, B.; Fang, L.; Huang, D.; and Qi, L. 2024. Learning attention in the frequency domain for flexible real photograph denoising. *IEEE Transactions on Image Processing*, 33: 3707–3721.
- Malarz, D.; Kasymov, A.; Zięba, M.; Tabor, J.; and Spurek, P. 2025. Classifier-free Guidance with Adaptive Scaling. *arXiv preprint arXiv:2502.10574*.
- Miyato, T.; Kataoka, T.; Koyama, M.; and Yoshida, Y. 2018. Spectral normalization for generative adversarial networks. *arXiv preprint arXiv:1802.05957*.
- Morelli, D.; Baldrati, A.; Cartella, G.; Cornia, M.; Bertini, M.; and Cucchiara, R. 2023. Ladi-vton: Latent diffusion textual-inversion enhanced virtual try-on. In *ACM International Conference on Multimedia*, 8580–8589.
- Morelli, D.; Fincato, M.; Cornia, M.; Landi, F.; Cesari, F.; and Cucchiara, R. 2022. Dress code: High-resolution multi-category virtual try-on. In *Computer Vision and Pattern Recognition*, 2231–2235.
- NASA. 2015. Pluto: The 'Other' Red Planet. <https://www.nasa.gov/nh/pluto-the-other-red-planet>. Accessed: 2018-12-06.
- Radford, A.; Kim, J. W.; Hallacy, C.; Ramesh, A.; Goh, G.; Agarwal, S.; Sastry, G.; Askell, A.; Mishkin, P.; Clark, J.; et al. 2021. Learning transferable visual models from natural language supervision. In *International Conference on Machine Learning*, 8748–8763.
- Ramesh, A.; Dhariwal, P.; Nichol, A.; Chu, C.; and Chen, M. 2022. Hierarchical text-conditional image generation with clip latents. *arXiv*, 1(2): 3.
- Rice, J. 1986. Poligon: A System for Parallel Problem Solving. Technical Report KSL-86-19, Dept. of Computer Science, Stanford Univ.
- Robinson, A. L. 1980a. New Ways to Make Microcircuits Smaller. *Science*, 208(4447): 1019–1022.
- Robinson, A. L. 1980b. New Ways to Make Microcircuits Smaller—Duplicate Entry. *Science*, 208: 1019–1026.
- Rombach, R.; Blattmann, A.; Lorenz, D.; Esser, P.; and Ommer, B. 2022. High-resolution image synthesis with latent diffusion models. In *Computer Vision and Pattern Recognition*, 10684–10695.
- Ronneberger, O.; Fischer, P.; and Brox, T. 2015. U-net: Convolutional networks for biomedical image segmentation. In *Medical Image Computing and Computer Assisted Intervention*, 234–241.
- Saharia, C.; Chan, W.; Saxena, S.; Li, L.; Whang, J.; Denton, E. L.; Ghasemipour, K.; Gontijo Lopes, R.; Karagol Ayan, B.; Salimans, T.; et al. 2022. Photorealistic text-to-image diffusion models with deep language understanding. *Advances in Neural Information Processing Systems*, 35: 36479–36494.
- Seitzer, M. 2020. pytorch-fid: FID Score for PyTorch. In *Computer Vision and Pattern Recognition*.
- Shen, D.; Song, G.; Xue, Z.; Wang, F.-Y.; and Liu, Y. 2024. Rethinking the spatial inconsistency in classifier-free diffusion guidance. In *Computer Vision and Pattern Recognition*, 9370–9379.
- Strang, G. 1993. Wavelet transforms versus Fourier transforms. *Bulletin of the American Mathematical Society*, 28(2): 288–305.
- Sun, K.; Cao, J.; Wang, Q.; Tian, L.; Zhang, X.; Zhuo, L.; Zhang, B.; Bo, L.; Zhou, W.; Zhang, W.; et al. 2024. Outfit anyone: Ultra-high quality virtual try-on for any clothing and any person. *arXiv*.
- Vaswani, A.; Shazeer, N.; Parmar, N.; Uszkoreit, J.; Jones, L.; Gomez, A. N.; Kaiser, L.; and Polosukhin, I. 2017. Attention Is All You Need. *arXiv:1706.03762*.
- Wang, Z.; Bovik, A. C.; Sheikh, H. R.; and Simoncelli, E. P. 2004. Image quality assessment: from error visibility to structural similarity. *IEEE Transactions on Image Processing*, 13(4): 600–612.
- Xie, Z.; Huang, Z.; Dong, X.; Zhao, F.; Dong, H.; Zhang, X.; Zhu, F.; and Liang, X. 2023. Gp-vton: Towards general purpose virtual try-on via collaborative local-flow global-parsing learning. In *Computer Vision and Pattern Recognition*, 23550–23559.
- Xu, Y.; Gu, T.; Chen, W.; and Chen, A. 2025. Ootdiffusion: Outfitting fusion based latent diffusion for controllable virtual try-on. In *AAAI Conference on Artificial Intelligence*, volume 39, 8996–9004.
- Yang, H.; Zhang, R.; Guo, X.; Liu, W.; Zuo, W.; and Luo, P. 2020. Towards photo-realistic virtual try-on by adaptively generating-preserving image content. In *Computer Vision and Pattern Recognition*, 7850–7859.
- Yang, X.; Ding, C.; Hong, Z.; Huang, J.; Tao, J.; and Xu, X. 2024. Texture-preserving diffusion models for high-fidelity virtual try-on. In *Computer Vision and Pattern Recognition*, 7017–7026.
- Ye, H.; Zhang, J.; Liu, S.; Han, X.; and Yang, W. 2023. Ip-adapt: Text compatible image prompt adapter for text-to-image diffusion models. *arXiv preprint arXiv:2308.06721*.
- Zhang, L.; Rao, A.; and Agrawala, M. 2023. Adding conditional control to text-to-image diffusion models. In *International Conference on Computer Vision*, 3836–3847.
- Zhang, R.; Isola, P.; Efros, A. A.; Shechtman, E.; and Wang, O. 2018. The unreasonable effectiveness of deep features as a perceptual metric. In *Computer Vision and Pattern Recognition*, 586–595.
- Zhou, M.; Huang, J.; Yan, K.; Yu, H.; Fu, X.; Liu, A.; Wei, X.; and Zhao, F. 2022. Spatial-frequency domain information integration for pan-sharpening. In *European Conference on Computer Vision*, 274–291.
- Zhou, Z.; Liu, S.; Han, X.; Liu, H.; Ng, K. W.; Xie, T.; Cong, Y.; Li, H.; Xu, M.; Pérez-Rúa, J.-M.; et al. 2025. Learning

flow fields in attention for controllable person image generation. In *Computer Vision and Pattern Recognition*, 2491–2501.

Zhu, L.; Yang, D.; Zhu, T.; Reda, F.; Chan, W.; Saharia, C.; Norouzi, M.; and Kemelmacher-Shlizerman, I. 2023. Tryon-diffusion: A tale of two unets. In *Computer Vision and Pattern Recognition*, 4606–4615.

## Appendix

### LS-TON Benchmark

Widely used public virtual try-on datasets—specifically VITON-HD (Choi et al. 2021) and DressCode (Morelli et al. 2022)—lack data curated for the long-sleeve-to-short-sleeve conversion task. Consequently, these datasets are inadequate for effectively evaluating VTON models in the more challenging scenario of long-sleeve to short-sleeve transformations. To address this gap, we introduce a new benchmark, LS-TON, specifically designed for long-sleeve to short-sleeve conversions. We curated image pairs from social platforms, consisting of models dressed in long-sleeved garments (e.g., heavy coats, padded jackets, and long-sleeved shirts) and short-sleeved clothing. Using multiple image editing tools, we manually replaced the long-sleeve garment in the model image with the short-sleeve garment, producing an image triplet: the source image (model wearing long sleeves), the reference image (short-sleeve garment), and the ground-truth (GT) image (model actually wearing the short-sleeve garment), as illustrated in Fig. 6. The resulting LS-TON dataset comprises 770 such triplets.

### Additional Experiments

**Experimental Settings Datasets.** We conduct experiments on two public fashion datasets, VITON-HD (Choi et al. 2021) and DressCode (Morelli et al. 2022), and a custom benchmark (LS-TON) for long-sleeve to short-sleeve try-on evaluation. VITON-HD contains 13,679 image pairs (11,647 training; 2,032 testing), each comprising a front-view upper-body photograph and its corresponding in-shop top at  $1024 \times 768$  resolution. DressCode contains 48,392 training and 5,400 testing pairs of full-body, front-view images paired with in-shop garments (tops, bottoms, and dresses), also at  $1024 \times 768$  resolution.

**Baselines.** We benchmark our proposed UR-VTON against several state-of-the-art diffusion-based virtual try-on models, including: GP-VTON (Xie et al. 2023) (part-wise garment warping for semantic and texture fidelity), LaDI-VTON (Morelli et al. 2023) (CLIP-based feature alignment and diffusion refinement), IDM-VTON (Choi et al. 2024) (cross-attention and parallel UNets for detail), OOTDiffusion (Xu et al. 2025) (fine-tuned garment UNet for denoising), CatVTON (Chong et al. 2025) (UNet simplification via spatial concatenation), and Leffa (Zhou et al. 2025) (attention flow regularization for artifact reduction and efficient portrait generation).

**Implementation Details.** The experiments are conducted on an Ubuntu 20.04.6 LTS system with the PyTorch framework, a single NVIDIA L20 GPU, and 45 GB of RAM. Unless otherwise specified, Leffa is used as the backbone for

UR-VTON in all subsequent experimental settings. The total number of timesteps  $T = 30$ , and guidance scale  $\omega = 2.5$ .

**Qualitative Comparison** To further demonstrate the effectiveness of UR-VTON, we qualitatively evaluated its performance on arbitrary garment-swap tasks by visually inspecting its virtual try-on results. As shown in Fig. 7 and 8, we test UR-VTON on challenging examples from two widely adopted high-resolution datasets—VITON-HD and DressCode—and compared it with several state-of-the-art methods to highlight differences in fine-grained consistency. Notably, baseline methods frequently exhibit garment transfer errors, visual artifacts, incoherent outputs, and detail loss, significantly limiting their practical applicability. In contrast, UR-VTON consistently produces accurate, natural garment transfers, underscoring its superior generalization and real-world applicability.

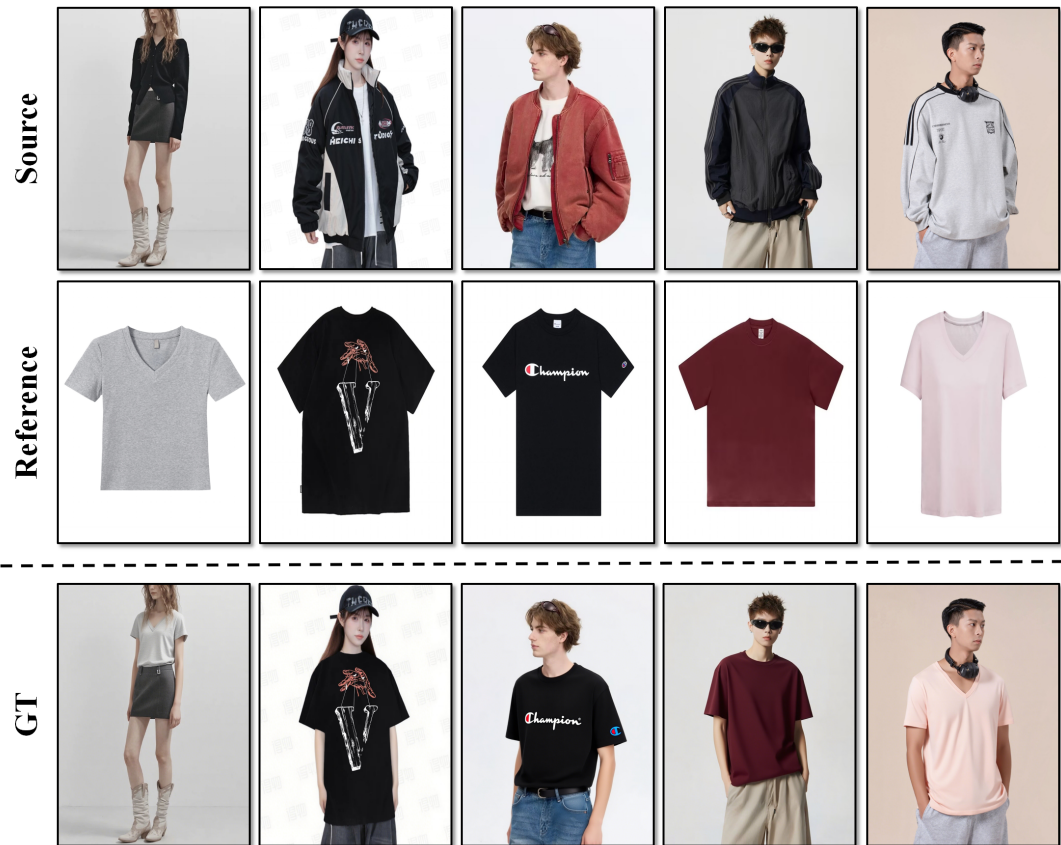


Figure 6: The overview of long-sleeve to short-sleeve try-on dataset.

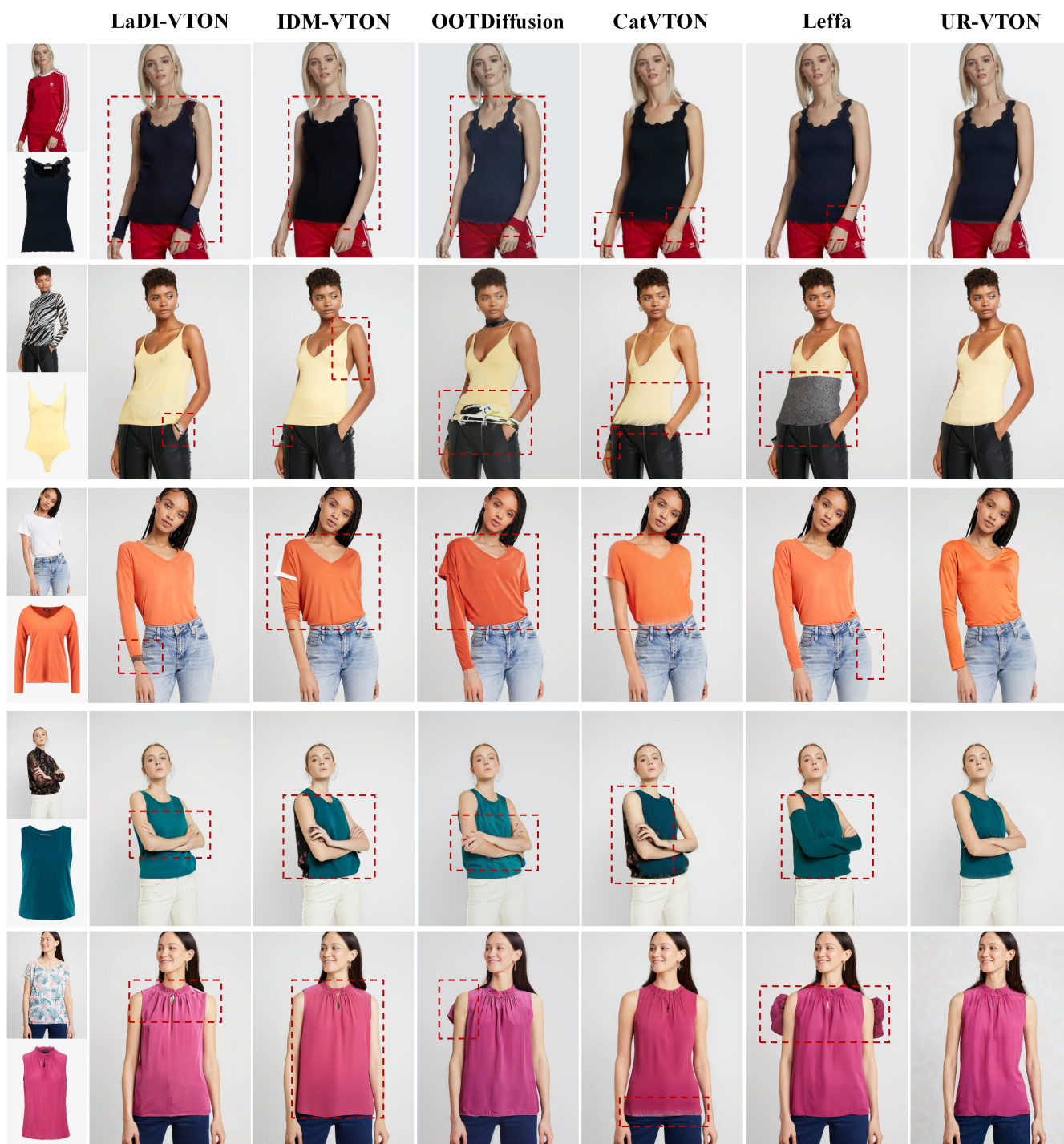


Figure 7: **Qualitative comparison on the VITON-HD dataset.** UR-VTON demonstrates significant advantages. We highlight the failure regions of the virtual try-on using red bounding boxes. Please zoom in to view more details.



Figure 8: **Qualitative comparison on the DressCode dataset.** UR-VTON demonstrates significant advantages. We highlight the failure regions of the virtual try-on using red bounding boxes. Please zoom in to view more details.